Nickel complexes of phosphine-appended benzannulated boron heterocycles

Laura A. Essex, Jordan W. Taylor, and W. Hill Harman*

Department of Chemistry, University of California, 501 Big Springs Rd. Riverside 92521

KEYWORDS: boranes, acceptor ligands, boron heterocycles

TOC Graphic:

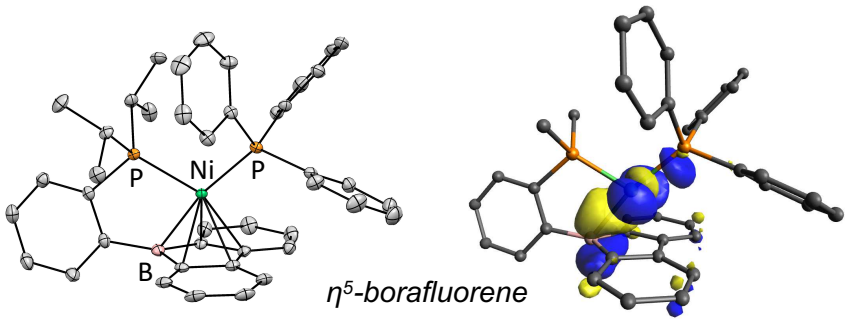

ABSTRACT: We report the synthesis and characterization of two diphosphine nickel complexes containing 9-borafluorene (PBFlu, 9-(diisopropylphosphino)phenyl-9-borafluorene) and 9,10-dihydroboranthrene (B_2P_2, 9,10-bis(2-(diisopropylphosphino)phenyl)-9,10-dihydroboranthrene) cores. Metalation of PBFlu and B_2P_2 with $Ni(PPh_3)_4$ leads to the monometallic complexes (PBFlu)Ni(PPh_3) and (B_2P_2)Ni, respectively. Cyclic voltammetry studies show a reversible redox event at ~ 0.1 V and a quasi-reversible event at ca. –3 V versus ferrocene/ferrocenium for (B_2P_2)Ni while (PBFlu)Ni(PPh_3) features no reversible redox events. Electronic structure calculations were performed to provide further insight into the bonding in these complexes.

Introduction

Boron for carbon substitution is a powerful method for modulating the properties of polycylic aromatic hydrocarbons (PAH), with applications in optoelectronic materials[1,2] and catalysis.[3] The empty p orbital on boron can act as a Lewis acid[4–7] or can introduce electron deficiency into the molecule, engendering facile multi-electron redox chemistry in many cases.[8] The boron substituted analogues of classic ligands such as cyclopentadienyl[9] and benzene[10] have been used to prepare a range of metal complexes with interesting electronic properties and chemical reactivity. They are of special interest given their potential to function as acceptor or Z-type ligands.[11–13]

The five-membered monoboron heterocycle borole (C_4H_4BH) is isoelectronic to the cyclopentadienyl cation and formally classified as an L_2Z ligand. The antiaromatic character of borole engenders significant reactivity in the molecule, and it has found applications in small molecule activation.[14] For example, perfluoropentaphenylborole is capable of cleaving dihydrogen[15] or undergoing Diels-Alder or insertion reactions with alkynes.[16] Reduced boroles can be stabilized by *N*-heterocyclic carbenes, conferring apparent boron-centered nucleophilicity.[17,18] The doubly benzannulated analogue of borole, 9-borafluorene (BFlu)[19] attenuates the anti-aromatic character of the central ring. BFlu derivatives have found applications as activators for transition metals.[20] Despite the rich chemistry of boron heterocycles as ligands, there are relatively few metal complexes of BFlu. Piers reported an adduct between a perfluoro-9-phenyl-9-borafluorene and Cp*Al,[21] and Bourissou used a phosphine-buttressed ligand (PBFlu, **1**) to prepare a BFlu complex exhibiting monohapto coordination through the boron, the first Au borane complex (Figure 1).[22]

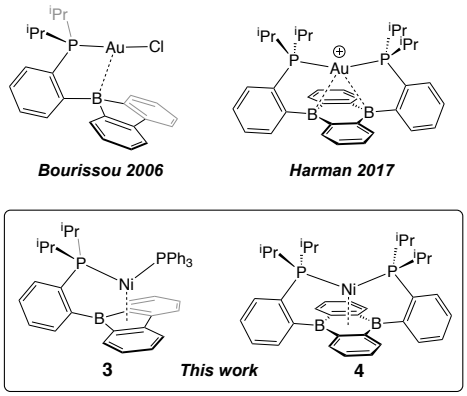

Figure 1. Previously reported Au complexes of PBFlu and B_2P_2 ligands (top). Ni complexes of PBFlu and B_2P_2 presented in this work (bottom).

The doubly benzannulated analogue of 9,10-dihydro-9,10-diborabenzene, 9,10-dihydro-9,10-diboraanthracene (DBA), is an electrochemically rich platform with broad synthetic flexibility and applications in organic electronic materials. Upon two electron reduction, Wagner has shown that DBA variants can cleave dihydrogen,[23] disproportionate CO_2,[24] break chalcogen-chalcogen bonds,[25] and activate sp C–H bonds.[26] We recently reported that NHC-stabilized 9,10-diboraanthracene undergoes formal [4+2] cycloaddition reactions at the boron centers with O_2, CO_2, and ethylene.[27] A number of electronically saturated metal complexes of DBA have been prepared, some of which contain multiple metal centers bound to a single DBA unit.[28] Due to the electron deficiency of DBA, oxidation of these complexes tends result in irreversible de-coordination of the ligand.[29]

We are interested in the emergent redox properties and chemical reactivity of metal complexes with heterocyclic boron-containing ligands. Recently, we reported the synthesis of a DBA-based ligand featuring two tethered phosphine donors straddling the central C_4B_2 ring (9,10-bis(2-(diisopropylphosphino)phenyl)-9,10-dihydroboranthrene, B_2P_2, **2**). Metal complexes of B_2P_2 can undergo DBA-centered redox events, as in the zwitterionic radical complexes $(B_2P_2)Cu$ and $(B_2P_2)Ag$ we recently described.[30] A series of Au complexes of B_2P_2 were also prepared in three states of charge, with the most reduced species, $[(B_2P_2)Au]^-$ being the first example of a molecular boroauride, featuring very short interactions between the Au atom and pyramidalized borons of the DBA core.[31] Given the intriguing chemistry uncovered for d^{10} coinage metal complexes with both PBFlu and B_2P_2, we investigated the related Ni complexes. Herein we report the synthesis, structure, NMR, and electrochemical characterization of the neutral Ni complexes of both **1** and **2**. Unlike their coinage metal analogues, these Ni complexes form penta- and hexahapto complexes, respectively, with the central boron heterocycles (Figure 1). Although the BFlu and DBA heterocycles have one and two borane centers, respectively, DFT calculations their Ni complexes are essentially isoelectronic and best described as d^{10} ML_4 Ni(0) complexes with a backbonding component (Z') into an empty orbital with boron character.

Scheme 1. Preparation of (PBFlu)Ni

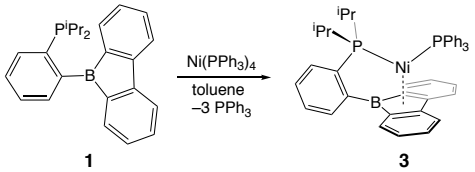

Results and Discussion

The phosphine-appended BFlu ligand **1** was first prepared by Bourissou and metalated *in situ* with $(Me_2S)AuCl$ without isolation of the ligand.[22] In our hands, lithiation of 2-(diisopropylphosphino)bromobenzene in toluene proceeds cleanly at –40 °C and the lithiated species is very stable in this solvent, even at room temperature. Subsequent addition of 9-bromo-9-borafluorene at –60°C results in a yellow solution that, upon warming to –20°C, changes to an intense red color, indicating near complete decomposition of the desired ligand. However, by avoiding warming reaction mixtures past –20 °C, **1** can be isolated as a colorless crystalline solid in low yields (16%) (Scheme 1). Once isolated, **1** is stable

at room temperature allowing its characterization by NMR spectroscopy. In solution, **1** exhibits a broad resonance centered at 0.9 ppm in the $^{11}B\{^{1}H\}$ NMR spectrum. For comparison, the ^{11}B resonance for 9-phenyl-9-borafluorene is 64.5 ppm, suggesting P–B interactions in **1**, although no ^{31}P–^{11}B coupling is observed (Scheme 1).[32]

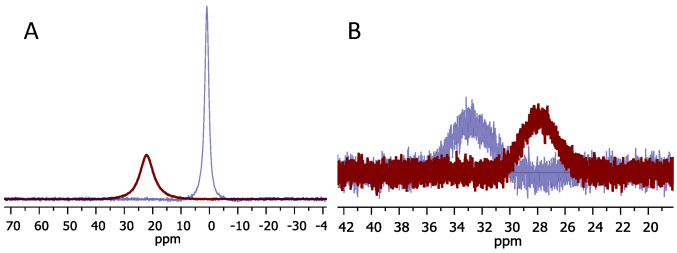

Figure 2. $^{11}B\{^{1}H\}$ NMR spectra of (A) PBFlu (**1**, blue) and (PBFlu)Ni (**3**, red); (B) B_2P_2 (**2**, blue) and $(B_2P_2)Ni$ (**4**, red).

Metalation of **1** with $Ni(PPh_3)_4$ affords the nickel complex (PBFlu)Ni (**3**), denoted by a downfield shift of the ^{11}B resonance to 22.5 ppm (Figure 2). Single-crystal X-ray diffraction (XRD) of **1** revealed an η^5-BFlu moiety coordinated to Ni with a Ni–B distance of 2.135(2) Å and Ni–C distances ranging from 2.217(2) to 2.230(2) Å (Figure 3). In contrast, the previously reported η^1-BFlu gold complex has a Au–B distance of 2.663(1) Å with no appreciable interaction between the Au center and other atoms of the BFlu unit (average $d_{Au\text{-}C\alpha} = 3.118(1)$ Å; $d_{Au\text{-}C\beta} = 3.750(1)$ Å) (Figure 3). While many η^5-borole complexes have been reported,[33–35] complex **3** is the first example of pentahapto coordination of BFlu.

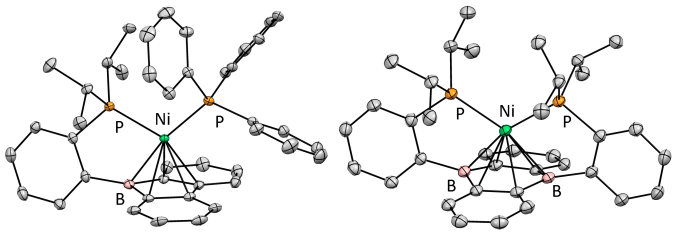

Figure 3. Labeled thermal ellipsoid plots (50%) of (PBFlu)Ni (3, left) and $(B_2P_2)Ni$ (**4**, right). Unlabeled ellipsoids correspond to carbon. Hydrogen atoms have been omitted for clarity.

The DBA-based ligand **2** allowed us to explore the effect of a second boron center in the coordination sphere of Ni. Metalation of **2** to give $(B_2P_2)Ni$ (**4**) can be achieved using either $Ni(PPh_3)_4$ or treating by a mixture of **2** and $NiBr_2$ with metallic Na (Scheme 2). In solution, **4** features a $^{11}B\{^{1}H\}$ resonance at 27.8 ppm that is shifted slightly upfield to that of the free ligand (34.1 ppm). Single-crystal XRD reveals η^6 coordination of Ni to the DBA core with an average Ni-B distance of 2.196(2) Å (Figure 3). In contrast, $[(B_2P_2)Au]^+$ has Au–B distances of 2.610(2) and 2.678(2) Å and no Au–C contact shorter than 2.75 Å.[31] These differences can be rationalized both by the prevalence of 14-electron Au(I) complexes as well as the stronger backbonding ability of Ni(0). We note that in all of the Ni complexes reported her, the boron centers are essentially planar (see Table 1).

Scheme 2. Synthesis of $(B_2P_2)Ni$

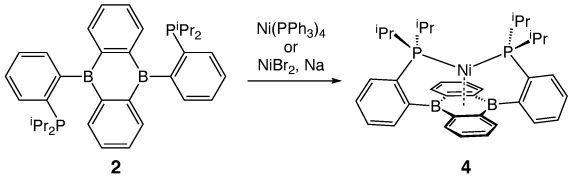

To further explore the electronic properties of these two complexes, we investigated their electrochemistry by cyclic voltammetry (CV). The CV of **2** features a single irreversible reduction at –3.00 V vs. Fc/Fc^+ with multiple irreversible events in the oxidative direction (Figure S17, S18). In contrast, **4** displays a reversible reduction event at −2.99 V vs. Fc/Fc^+ and an electrochemically slow but chemically reversible oxidation at +0.06 V (Figure S19). It is instructive to compare the electrochemistry of **2** and **4** to

that of the corresponding free ligands **1** and **3**. The CV of **1** displays a reversible reduction at –2.09 and an irreversible reduction at –2.70 V. The irreversibility of the second reduction may be due to reductive cleavage of the endocyclic B–C bond, a phenomenon that has been observed in boroles and related molecules.[16,36,37] In contrast, **2** undergoes reversible reductions at –2.18 and –2.71 V vs. Fc/Fc^+. In both cases, the free ligands are more easily reduced than the corresponding Ni complexes, consistent with strong donation from a filled Ni d-orbital into the empty boron-based orbitals on the BFlu and DBA fragments. These results are counter to what we have observed in the cases of the coinage metal complexes of **3** $[(B_2P_2)M]^+$ (M = Cu, Ag, Au), all of which are easier to reduce than free **3** (Table 1). The positive charge on the coinage metal complexes is likely a significant contributor to this observation.

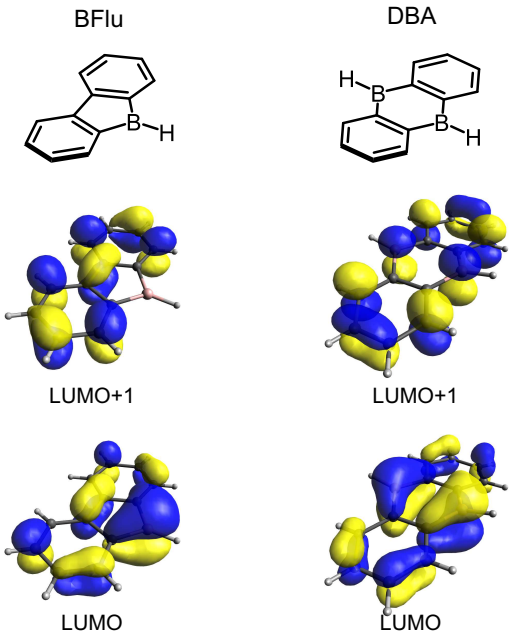

Figure 4. The two lowest energy unoccupied Kohn-Sham orbitals calculated for BFlu (left) and DBA (right, see SI for computational details).

DFT calculations were carried out on truncated models[38] of **2** and **4** as well as BFlu and DBA to shed light on the interaction between the Ni center and the boron heterocycles. The two lowest energy unoccupied orbitals for BFlu and DBA are shown in Figure 4 and reveal that in both cases, the LUMO has significant boron character. In the case of DBA, this orbital is composed of the out-of-phase combination of the two boron p orbitals. This orbital is analogous to the HOMO of anthracene and has overall bonding character. The second unoccupied molecular orbital in DBA (LUMO+1) corresponds to the in-phase combination of the empty boron p-orbitals. As this orbital is analogous to the LUMO of anthracene, it is antibonding. Although there are in principle two relevant acceptor orbitals in DBA, the in-phase combination of the boron p orbitals (LUMO+1) is significantly higher in energy than the out-of-phase combination (LUMO) due to the antibonding nature of the former and bonding nature of the latter. The five highest energy occupied molecular orbitals of **2** and **4** are shown in Figures 5 and 6, respectively. In both cases, the five highest energy filled orbitals have significant if not predominantly d-character, consistent with a d^{10} Ni(0) description. In **3**, the Ni–B acceptor interaction serves to stabilize an orbital of d parentage that is antibonding with respect to the Ni–PPh_3 interaction (HOMO–2). In **4** the primary molecular orbital featuring Ni–B bonding is also the HOMO–2, which consists of the in-phase combination of a Ni d orbital and the LUMO of DBA described above. The HOMO–1 in **4** contains a small component of the in-phase combination of the boron p orbitals, corresponding to the LUMO+1 of DBA. This interaction is less pronounced, owing to the higher energy of the DBA LUMO+1 (in-phase boron p orbitals) relative to the LUMO (out-of-phase boron p orbitals). For these reasons, we favor a description of both BFlu and DBA in **2** and **4** as L_2 ligands with a significant backbonding component associated with the boron p orbitals. In both cases, the d-orbital splittings can be rationalized as perturbations on an approximately tetrahedral ligand field.

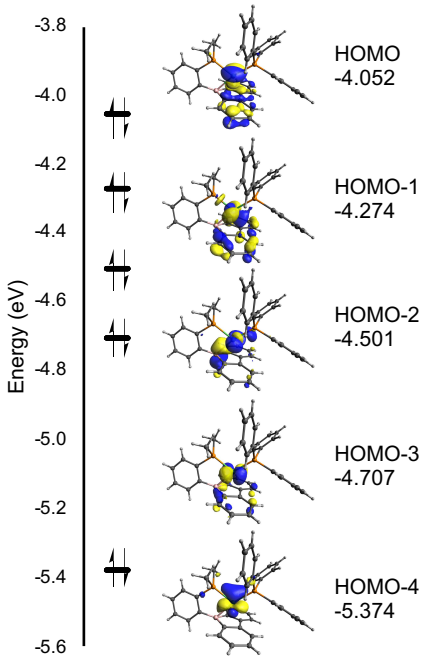

Figure 5. The five highest energy occupied Kohn-Sham orbitals calculated for a truncated model of (PBFlu)Ni (**2**).

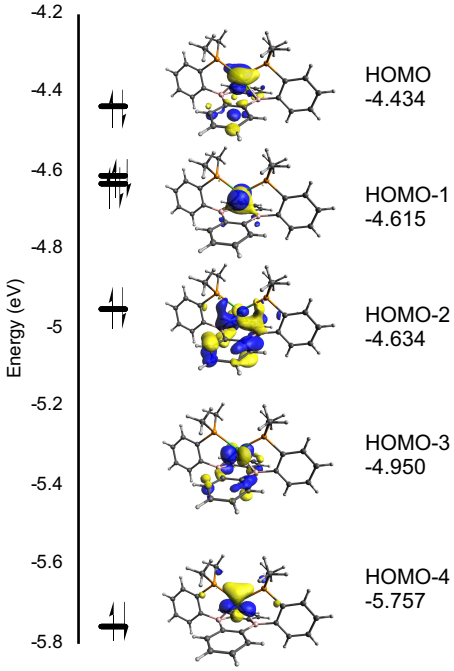

Figure 6. The five highest energy occupied Kohn-Sham orbitals calculated for a truncated model of (B_2P_2)Ni (**4**).

Conclusion

In summary, we have synthesized two new nickel complexes **2** and **4** featuring strong interactions of the Ni center with boron heterocycles. The interaction between Ni and the boron heterocycles in these complexes is much more pronounced than in the analogous complexes of the coinage metal cations. Where the coinage metal complexes are easier to reduce than the corresponding free ligands, **2** and **4** are significantly more difficult, consistent with strong backbonding of the Ni center into the boron-based orbitals of the heterocycles. DFT calculations on **2** and **4** are consistent with this description. The five highest energy orbitals in both **2** and **4** have significant d character, with the HOMO–2 in both cases possessing Ni–B bonding interactions. Given the presence of the Ni–B bonding orbital in the middle of the d manifold, a d^{10} electron count is appropriate for these complexes, wherein the Ni–B interaction is best described as backbonding.

Table 1. Selected bonds, angles, ^{11}B NMR data and CV data for PBFlu, B_2P_2 and their transition metal complexes

Compound	^{11}B [ppm]	M–B_{avg} [Å]	M–C_{avg} [Å]	ΣB_α [°]	$E_{1/2}$ [V]
PBFlu	0.90				–2.09[b], –2.70[c]
B_2P_2	34.1				–2.18, –2.71
(PPh_3)Ni(PBFlu)	22.5	2.316	2.233, 2.216[a]	360.0	–3.00[c]
Ni(B_2P_2)	27.8	2.196	2.349	360.0	0.06, –2.99[b]
[Cu(B_2P_2)][BAr^F_4]	47.2	2.372	2.514	360.0	–1.66[b]
[Ag(B_2P_2)][BAr^F_4]	29.2	2.567	2.730	360.0	–1.56, –2.21[c]
Ag(B_2P_2)		2.892	2.985	359.9	
[Au(B_2P_2)][BAr^F_4]	32.0	2.644	2.832	360.0	–1.60, –2.05
Au(B_2P_2)		3.049	3.189	360.0	
[Au(B_2P_2)][K(18-c-6)]	11.1	2.239		343.9	

[a]The averages are taken between the two crystallographically distinct molecules of (PPh_3)Ni(PBFlu) in the unit cell and are listed in the order of alpha and beta to denote the slight asymmetry about the Ni-BC_4 unit
[b]This process was quasi-reversible on the CV timescale (100 mV/s scan rate)
[c]This process was irreversible on the CV timescale (100 mV/s scan rate)

Experimental Section

General considerations. Unless otherwise noted, all manipulations were carried out using standard Schlenk or glovebox techniques under a N_2 atmosphere. Hexanes, benzene, toluene, and acetonitrile were dried and deoxygenated by argon sparge followed by passage through activated alumina in a solvent purification system from JC Meyer Solvent Systems followed by storage over 4 Å molecular sieves. THF and Et_2O were distilled from sodium-benzophenone ketyl under N2 followed by storage over 4Å molecular sieves for at least 24 hours prior to use. Non-halogenated and non-nitrile containing solvents were tested with a standard purple solution of sodium benzophenone ketyl in THF to confirm effective oxygen and moisture removal prior to use. Hexamethyldisiloxane (HMDSO) was distilled from sodium metal and stored over 4Å molecular sieves for 24 hours prior to use. All reagents were purchased from commercial suppliers and used without further purification unless otherwise noted. 9-bromo-9-borafluorene,[39] 2-(diisopropylphosphino)bromobenzene,[22] and 9,10-bis(2-(diisopropylphosphino)phenyl)-9,10-dihydroboranthrene (B_2P_2, **2**)[31] were synthesized according to literature procedures. Elemental analyses were performed by Midwest Microlab, LLC, Indianapolis, IN. Deuterated solvents were purchased from Cambridge Isotope Laboratories Inc., degassed, and dried over activated 3Å molecular sieves for at least 24 h prior to use. NMR spectra were recorded on Bruker Neo 400 MHz, and Bruker Avance 600 MHz spectrometers. ^{1}H and ^{13}C chemical shifts are reported in ppm relative to tetramethylsilane using residual solvent as an internal standard. ^{11}B chemical shifts are reported in ppm relative to BF_3•Et_2O. Original ^{11}B NMR spectra were processed using MestReNova 11.0.2 with a backwards-linear prediction applied to eliminate background signal from the borosilicate NMR tube. For ^{11}B NMR spectra with peaks overlapping the borosilicate signal, a manual baseline correction was applied. UV-Vis spectra were recorded using a Cary Bio 500 spectrometer using a 1 cm path length quartz cuvette with a solvent background subtraction applied. X-ray diffraction studies were performed using a Bruker-AXS diffractometer. Cyclic Voltammetry (CV) experiments were performed using a Pine AFP1 potentiostat. The cell consisted of a glassy carbon working electrode, a Pt wire auxiliary electrode and a Pt wire pseudo-reference electrode. All potentials are referenced vs. the Fc/Fc^+ couple measured as an internal standard. Calculations were run using Orca v4.0.1 and visualized with Avogadro v1.2.0.

9-(2-(diisopropylphosphino)phenyl)-9-borafluorene (1). Using a modified procedure from Bourissou *et al*. n-BuLi (2.5 M in hexanes, 2.5 mL, 6.25 mmol) and 9-bromo-borafluorene (1.5 g, 6.2 mmol) were successively added at –40 °C and –60 °C to a solution of 1-bromo-2-diisopropylphosphinobenzene (1.5 g, 5.5 mmol) in toluene (80 mL).[22] The suspension was pumped down to a pale orange solid and brought into the glovebox. The solid was re-suspended in toluene (80 mL) that had been pre-chilled to –50°C and filtered through celite at the same temperature. The filtrate was concentrated *in vacuo* and layered with hexanes, providing colorless crystals. Yield: 0.311 g (16%). ^{1}H NMR (400 MHz, C_6D_6) δ 7.87 (dd, *J* = 7.5, 0.9 Hz, 2H), 7.49 (dd, *J* = 7.2, 2.3 Hz, 2H), 7.36 (tdd, *J* = 7.5, 2.5, 1.3 Hz, 2H), 7.26 – 7.17 (m, 4H), 7.14 – 7.08 (m, 2H), 2.15 (dp, *J* = 9.3, 7.3 Hz, 2H), 0.80 (d, *J* = 7.1 Hz, 3H), 0.77 (d, *J* = 7.2 Hz, 3H), 0.73 (d, *J* = 7.4 Hz, 3H), 0.69 (d, *J* = 7.4 Hz, 3H).^{13}C{^{1}H} NMR (101 MHz, C_6D_6) δ 164.8 (br), 153.2 (br), 149.7 (d, *J* = 4.7 Hz), 136.1 (d, *J* = 48.1 Hz), 132.3 (d, *J* = 2.6 Hz), 131.4 (d, *J* = 39.0 Hz), 131.3 (d, *J* = 3.8 Hz), 127.2 (d, *J* = 3.5 Hz), 127.1, 125.8 (d, *J* = 3.7 Hz), 119.7 (d, *J* = 2.4 Hz), 23.5 (d, *J* = 8.5

Hz), 18.4, 18.0. $^{11}B\{^1H\}$ NMR (128 MHz, C_6D_6) δ 0.9. ^{31}P NMR (162 MHz, C_6D_6) δ 33.0. HRMS (ESI): *m/z* for $C_{24}H_{27}BP$ $[M+H]^+$ calcd.: 357.1938, found: 357.1978.

(PBFlu)Ni(PPh$_3$) (3). A solution of **1** (69 mg, 0.19 mmol) in toluene (4 mL) was added to a stirring solution of tetrakis(triphenylphosphine)nickel(0) (213 mg, 0.19 mmol) in toluene (10 mL). After 2 hours, the solution was concentrated *in vacuo* and layered with hexane (2 mL), providing burgundy-brown crystals of **2** that were washed with hexanes (2 x 3 mL) and dried *in vacuo*. Crystals suitable for XRD can be generated from layering hexane over toluene or ether over THF. Yield: 0.120 g (91%). ^1H NMR (400 MHz, C_6D_6) δ 7.97 (d, *J* = 7.3 Hz, 1H), 7.66 (d, *J* = 7.6 Hz, 2H), 7.40 (tdd, *J* = 7.4, 2.5, 1.2 Hz, 1H), 7.21 (dddd, *J* = 9.5, 7.3, 4.9, 2.3 Hz, 7H), 7.14 – 7.07 (m, 3H), 7.07 – 6.96 (m, 11H), 6.51 (d, *J* = 8.0 Hz, 2H), 1.17 (h, *J* = 7.2 Hz, 2H), 0.85 (d, *J* = 7.0 Hz, 3H), 0.81 (d, *J* = 7.0 Hz, 3H), 0.53 (d, *J* = 7.1 Hz, 3H), 0.49 (d, *J* = 7.0 Hz, 3H). $^{13}C\{^1H\}$ NMR (101 MHz, C_6D_6) δ 155.8, 144.8 (dd, *J* = 40.4, 15.1 Hz), 134.8, 134.6, 134.5 (d, *J* = 9.7 Hz), 131.9 (dd, *J* = 24.1, 2.7 Hz), 131.2, 129.9, 129.3, 129.2 (d, *J* = 2.5 Hz), 127.7, 127.7, 126.2 (d, *J* = 2.9 Hz), 125.7 (d, *J* = 5.6 Hz), 123.6, 121.1, 119.0 (d, *J* = 2.8 Hz), 114.9, 25.6 (d, *J* = 19.3 Hz), 19.3 (d, *J* = 5.6 Hz), 17.8. $^{11}B\{^1H\}$ NMR (128 MHz, C_6D_6) δ 22.5. ^{31}P NMR (162 MHz, C_6D_6) δ 55.7 (d, *J* = 24.2 Hz), 36.7 (d, *J* = 24.2 Hz). UV-vis (Benzene) λ_{max} (nm) (ε_{max} ($M^{-1}cm^{-1}$)) 560 (sh, 3.2 x 10^2), 417 (sh, 3.5 x 10^3). Anal. Calcd. for $C_{36}H_{44}B_2NiP_2$ (1 x $C_4H_{10}O$): C, 73.73 H, 6.59. Found: C, 73.47 H, 5.95.

(B$_2$P$_2$)Ni (4).

Via NiBr$_2$: A solution of B_2P_2 (0.200 g, 0.357 mmol) in THF (3 mL) was added to a slurry of $NiBr_2$ (0.080 g, 0.366 mmol) in THF (3 mL) and stirred 4 hours. The orange/red mixture had its volatiles removed, was added Et_2O (5 mL) and again had its volatiles removed. The remaining orange/red foam was extracted with toluene (2 x 3 mL) and filtered through celite into a 20 mL vial containing sodium (0.021 g, 0.893 mmol). The solution was stirred 10 hours during which time a deep red solution formed. The mixture was filtered through celite and concentrated to ca. 2 mL before adding Et_2O (5 mL). The mixture was filtered through a 1" pad of silica gel and rinsed with toluene:Et_2O (2:5, 10 mL). Removal of the volatiles gave the product as a red solid. Overall yield: 0.157 g, 71%.

Via Ni(PPh$_3$)$_4$: A solution of B_2P_2 (0.200 g, 0.357 mmol) in THF (5 mL) was added to $Ni(PPh_3)_4$ (0.395 g, 0.357 mmol) in THF (3 mL) and the mixture stirred at 50 °C for 12 hours. The deep red solution had its volatiles removed *in vacuo* before dissolving the residue in THF:Et_2O (1:9, 10 mL) and passing it through a 1" pad of silica. Removal of the volatiles *in vacuo* gave the product as a red/orange solid. Overall yield: 0.197 g, 89%. X-ray quality crystals were grown by layering a concentrated toluene solution with MeCN. ^1H NMR (500 MHz, C_6D_6) δ 8.01 (d, *J* = 7.2 Hz, 2H), 7.62 (apparent dd, *J* = 5.9, 3.4 Hz, 4H), 7.48 (t, *J* = 7.2 Hz, 2H), 7.36 – 7.30 (m, 2H), 7.27 (t, *J* = 7.5 Hz, 2H), 7.11 (apparent dd, *J* = 6, 3.4 Hz, 4H), 2.04 (dp, *J* = 14.2, 7.3 Hz, 4H), 0.74 (d, *J* = 6.9 Hz, 6H), 0.72 (d, *J* = 6.9 Hz, 6H), 0.61 (d, *J* = 7.1 Hz, 6H), 0.58 (d, *J* = 7.1 Hz, 6H). ^{31}P (202 MHz, C_6D_6) δ 45.6 (s). $^{11}B\{^1H\}$ (160 MHz) δ 27.8 (bs). $^{13}C\{^1H\}$ NMR (126 MHz, C_6D_6) δ 159.3, 143.1-142.9 (m), 135.0, 132.0 – 131.4 (m), 130.6, 130.1, 129.9, 126.9, 125.4, 27.7 (apparent dt, *J* = 18.3, 8.5 Hz), 20.0, 18.9. UV-vis (THF): λ_{max} (nm) (ε_{max} ($M^{-1}cm^{-1}$)) 318 (sh, 2.5 x 10^4), 372 (1.7 x 10^4), 451 (7.9 x 10^3), 577 (sh, 2.8 x 10^3). Anal. Calcd. for $C_{36}H_{44}B_2NiP_2$ (1 x $C_4H_{10}O$): C, 69.31 H, 7.85. Found: C, 69.98 H, 8.62.

Acknowledgements

This research was supported by the National Science Foundation (CHE-1752876) and the American Chemical Society Petroleum Research Fund (57314-DNI3). NMR spectra were collected on instruments funded by an NSF MRI grant (CHE-1626673) and an Army Research

Office instrumentation grant (W911NF-16-1-0523). We thank Dr. Fook Tham for assistance with X-ray crystallographic studies.

Appendix A. Supplementary data

Crystallographic data for **3** and **4** have been uploaded to the Cambridge Structural Database under accession numbers CCDC 1885406 and CCDC 1885407.

References

(1) Agnoli, S.; Favaro, M. *J. Mater. Chem. A* **2016**, *4* (14), 5002–5025.
(2) Escande, A.; Ingleson, M. J. *Chem. Commun.* **2015**, *51* (29), 6257–6274.
(3) Grimes, R. N. In *Comprehensive Organometallic Chemistry III*; Elsevier, 2007; pp 1–48.
(4) Kessler, S. N.; Wegner, H. A. *Org. Lett.* **2010**, *12* (18), 4062–4065.
(5) Emslie, D. J. H.; Piers, W. E.; Parvez, M. *Angew. Chemie Int. Ed.* **2003**, *42* (11), 1252–1255.
(6) Lorbach, A.; Bolte, M.; Lerner, H.-W.; Wagner, M. *Chem. Commun.* **2010**, *46* (20), 3592.
(7) Matsuo, K.; Saito, S.; Yamaguchi, S. *J. Am. Chem. Soc.* **2014**, *136* (36), 12580–12583.
(8) Reus, C.; Weidlich, S.; Bolte, M.; Lerner, H.-W.; Wagner, M. *J. Am. Chem. Soc.* **2013**, *135* (34), 12892–12907.
(9) Herberich, G. E.; He�ner, B.; Boveleth, W.; L�the, H.; Saive, R.; Zelenka, L. *Angew. Chemie Int. Ed. English* **1983**, *22* (S12), 1503–1510.
(10) Herberich, G. E.; Ohst, H. *Adv. Organomet. Chem.* **1986**, *25*, 199–236.
(11) Amgoune, A.; Bourissou, D. *Chem. Commun.* **2011**, *47* (3), 859–871.
(12) Braunschweig, H.; Dewhurst, R. D. *Dalt. Trans.* **2011**, *40* (3), 549–558.
(13) Emslie, D. J. H.; Cowie, B. E.; Kolpin, K. B. *Dalt. Trans.* **2012**, *41* (4), 1101–1117.
(14) Braunschweig, H.; Kupfer, T. *Chem. Commun.* **2011**, *47* (39), 10903.
(15) Fan, C.; Mercier, L. G.; Piers, W. E.; Tuononen, H. M.; Parvez, M. *J. Am. Chem. Soc.* **2010**, *132* (28), 9604–9606.
(16) Fan, C.; Piers, W. E.; Parvez, M.; McDonald, R. *Organometallics* **2010**, *29* (21), 5132–5139.
(17) Braunschweig, H.; Chiu, C.-W.; Radacki, K.; Kupfer, T. *Angew. Chemie Int. Ed.* **2010**, *49* (11), 2041–2044.
(18) Bertermann, R.; Braunschweig, H.; Dewhurst, R. D.; Hörl, C.; Kramer, T.; Krummenacher, I. *Angew. Chem. Int. Ed. Engl.* **2014**, *53* (21), 5453–5457.
(19) Köster, R.; Benedikt, G. *Angew. Chemie* **1963**, *75* (9), 419–419.
(20) Chase, P. A.; Piers, W. E.; Patrick, B. O. *J. Am. Chem. Soc.* **2000**, *122* (51), 12911–12912.
(21) Romero, P. E.; Piers, W. E.; Decker, S. A.; Chau, D.; Woo, T. K.; Parvez, M. *Organometallics* **2003**, *22* (6), 1266–1274.
(22) Bontemps, S.; Bouhadir, G.; Miqueu, K.; Bourissou, D. *J. Am. Chem. Soc.* **2006**, *128* (37), 12056–12057.
(23) von Grotthuss, E.; Diefenbach, M.; Bolte, M.; Lerner, H.-W.; Holthausen, M. C.; Wagner, M. *Angew. Chemie Int. Ed.* **2016**, *55* (45), 14067–14071.
(24) von Grotthuss, E.; Prey, S. E.; Bolte, M.; Lerner, H.-W.; Wagner, M. *Angew. Chemie Int. Ed.* **2018**, *57* (50), 16491–16495.
(25) von Grotthuss, E.; Nawa, F.; Bolte, M.; Lerner, H.-W.; Wagner, M. *Tetrahedron* **2019**, *75* (1), 26–30.
(26) Lorbach, A.; Bolte, M.; Lerner, H.-W.; Wagner, M. *Organometallics* **2010**, *29* (22), 5762–5765.
(27) Taylor, J. W.; McSkimming, A.; Guzman, C. F.; Harman, W. H. *J. Am. Chem. Soc.* **2017**,

139 (32), 11032–11035.
(28) Müller, P.; Pritzkow, H.; Siebert, W. *J. Organomet. Chem.* **1996**, *524* (1–2), 41–47.
(29) Müller, P.; Gangnus, B.; Pritzkow, H.; Schulz, H.; Stephan, M.; Siebert, W. *J. Organomet. Chem.* **1995**, *487* (1–2), 235–243.
(30) Taylor, J. W.; McSkimming, A.; Moret, M.-E.; Harman, W. H. *Inorg. Chem.* **2018**, acs.inorgchem.8b02710.
(31) Taylor, J. W.; McSkimming, A.; Moret, M.-E.; Harman, W. H. *Angew. Chemie Int. Ed.* **2017**, *56* (35), 10413–10417.
(32) Bontemps, S.; Bouhadir, G.; Dyer, P. W.; Miqueu, K.; Bourissou, D. *Inorg. Chem.* **2007**, *46* (13), 5149–5151.
(33) Herberich, G. E.; Hessner, B.; Ohst, H.; Raap, I. A. *J. Organomet. Chem.* **1988**, *348* (3), 305–316.
(34) Herberich, G. E.; Carstensen, T.; Koeffer, D. P. J.; Klaff, N.; Boese, R.; Hyla-Kryspin, I.; Gleiter, R.; Stephan, M.; Meth, H.; Zenneck, U. *Organometallics* **1994**, *13* (2), 619–630.
(35) Herberich, G. E.; Eckenrath, H. J.; Englert, U. *Organometallics* **1998**, *17* (4), 519–523.
(36) Shoji, Y.; Tanaka, N.; Muranaka, S.; Shigeno, N.; Sugiyama, H.; Takenouchi, K.; Hajjaj, F.; Fukushima, T. *Nat. Commun.* **2016**, *7* (1), 12704.
(37) Bluer, K. R.; Laperriere, L. E.; Pujol, A.; Yruegas, S.; Adiraju, V. A. K.; Martin, C. D. *Organometallics* **2018**, *37* (17), 2917–2927.
(38) Isopropyl groups were simplified to methyls.
(39) Berger, C. J.; He, G.; Merten, C.; McDonald, R.; Ferguson, M. J.; Rivard, E. *Inorg. Chem.* **2014**, *53* (3), 1475–1486.